Virologica Sinica 38 (2023) 309–312

Contents lists available at ScienceDirect

Virologica Sinica

journal homepage: www.keaipublishing.com/en/journals/virologica-sinica
www.virosin.org

Letter

Genome-wide characterization of alternative splicing in blood cells of COVID-19 and respiratory infections of relevance

Rui Huang [a,1], Wenbo Chen [b,1], Xueya Zhao [c,1], Yuefei Ma [e], Qiong Zhou [f], Junsen Chen [a], Muyi Zhang [a], Dingran Zhao [a], Yu Hou [d], Chunjiang He [b,*], Ying Wu [a,*]

[a] State Key Laboratory of Virology and Hubei Province Key Laboratory of Allergy and Immunology, Institute of Medical Virology, TaiKang Medical School, Wuhan University, Wuhan, 430072, China
[b] TaiKang Medical School, Wuhan University, Wuhan, 430071, China
[c] Institute of Life Sciences, Chongqing Medical University, Chongqing, 400016, China
[d] Tongji Hospital, Tongji Medical College, Huazhong University of Science and Technology, Wuhan, 430030, China
[e] Department of Clinical Laboratory, The First Affiliated Hospital, Fujian Medical University, Fuzhou, 350005, China
[f] Public Health Institute of Kunming Medical University, Kunming, 650500, China

Dear Editor,

Alternative splicing of eukaryotic transcripts refers to the post-transcriptional process in which the coding regions (exons) of a precursor transcript are joined in different combinations through the removal or retention of non-coding intervening sequences (introns) to produce distinct mature messenger RNA (mRNA) transcripts and further generate one or more mature mRNAs (Lee and Rio, 2015). Alternative splicing is revealed dysregulation in infectious diseases. Many pathogens hijack the splicing mechanism of host cells to complete their replications, accompanied by dysregulated innate immune response or cell damage, leading to the changes of alternative splicing landscape in host cells (Ashraf et al., 2019; Tomezsko et al., 2020; Kremsdorf et al., 2021). The regulation mechanism of alternative splicing by viral pathogens, such as hepatitis B virus (Duriez et al., 2017), human immunodeficiency virus 1 (Tomezsko et al., 2020), Zika virus (Bonenfant et al., 2020) and enterovirus 71 (Li et al., 2020), have been explored.

The common pathogens causing pneumonia in clinic include bacteria, mycoplasma and virus, such as Klebsiella pneumoniae, SARS-CoV-2, seasonal coronaviruses and influenza virus. Though the transcriptomic changes of SARS-CoV-2 have been frequently investigated (Zheng et al., 2020; McClain et al., 2021), the global view of alternative splicing events during SARS-CoV-2 infection is still lacking, and the mechanisms of altered cellular transcriptomic profiling in virus pathogenesis and host immune responses remain largely unknown. Here, we re-analyzed the public RNA-Seq datasets of human whole blood (McClain et al., 2021, GSE161731), and performed a comprehensive transcriptome-wide analysis of alternative splicing in a cohort of patients covering five groups of infections, including SARS-CoV-2 (severe and mild), seasonal coronaviruses, influenza and bacterial pneumonia (Fig. 1A). The detailed methods and procedures can be found in the supplementary materials.

Alternative splicing events (ASEs) are found to exhibit specificity and similarity among COVID-19 and other respiratory diseases in the distribution of differential alternative splicing events (DASEs), the length of intron fragments, as well as the enrichment of pathways such as metabolism, immunity and inflammation. A total of 4602 upregulated and 5420 downregulated DASEs are observed in severe COVID-19, mild COVID-19, bacterial pneumonia, seasonal coronaviruses pneumonia, influenza pneumonia groups, of which 1299, 937, 452, 174 and 1740 DASEs are significantly upregulated, while 2100, 1206, 374, 173 and 1567 DASEs are significantly downregulated respectively in these five groups (Fig. 1B, Supplementary Table S1). Similarity analysis of DASEs indicated relatively higher similarity scores between SARS-CoV-2 (Mild) and seasonal coronavirus (0.60 and 0.73 in up and downregulated DASEs respectively). Influenza and seasonal coronavirus exhibited high similarity scores: 0.64 and 0.59 in up- and down-regulated DASEs respectively, which were higher than other comparing groups. In contrast, bacterial group and seasonal coronavirus group exhibited relatively lower similarity scores: both 0.31 in up and downregulated DASEs (Supplementary Fig. S1A). Five splicing patterns, including exon skipping (SE), mutually exclusive exons (MXE), retained intron (RI), alternative 3′ splice site (A3SS) and alternative 5′ splice site (A5SS), are analyzed and the results are shown in Supplementary Fig. S1B. The size and location of the flanking introns are involved in splicing site recognition (Fox-Walsh et al., 2005). We inspected the distribution of intron

* Corresponding authors.
E-mail addresses: che@whu.edu.cn (C. He), yingwu@whu.edu.cn (Y. Wu).
[1] Rui Huang, Wenbo Chen, and Xueya Zhao contributed equally to this work.

https://doi.org/10.1016/j.virs.2023.01.007
Received 14 July 2022; Accepted 30 December 2022
Available online 20 January 2023

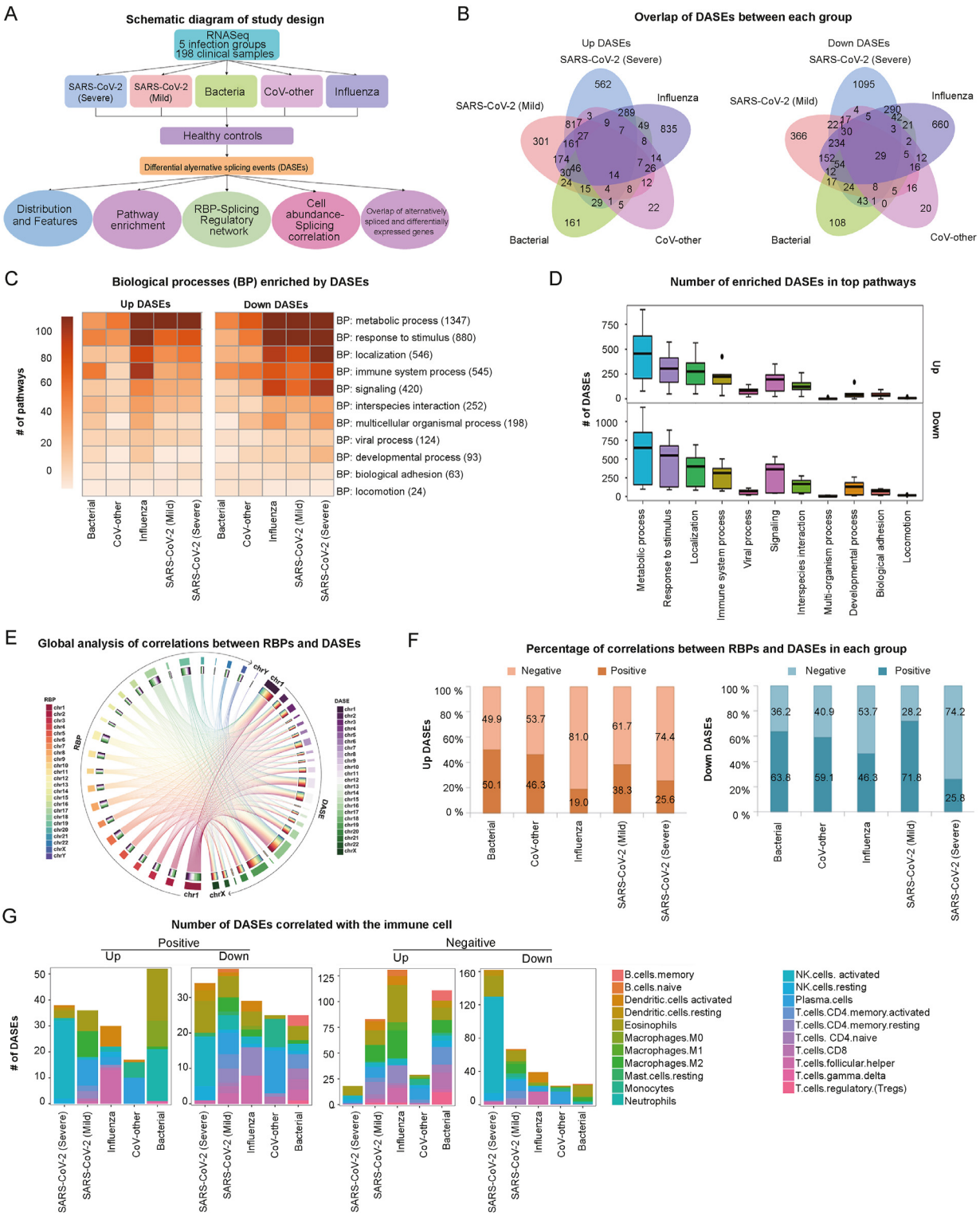

Fig. 1. Genome-wide characterization of alternative splicing of COVID-19 and respiratory infections of relevance in human blood cells. **A** Schematic diagram of study design. RNA-Seq of 198 samples from severe COVID-19, mild COVID-19, bacterial pneumonia, seasonal coronaviruses pneumonia, influenza pneumonia groups and healthy control were used to identify different alternative splicing events and perform comparison analysis of splicing features, functional pathways, regulation of RNA binding protein (RBP), cell abundance related to pathogen infection and overlap of alternatively spliced and differentially expressed genes. **B** Overlap of differential alternative splicing events (DASEs) between five infection groups. Up and down DASEs represent events upregulated and downregulated in infection groups were compared to healthy controls, separately. **C** Biological processes (BP) enriched by DASEs. The number of top biological processes enriched by DASEs of five infection groups was showed. **D** Top pathways enriched by DASEs of five infection groups. The number of DASEs enriched in top pathways was showed. **E** Circos plot depicting the significant correlation of all RBPs and DASEs in five groups. **F** Correlation analysis between RBPs and DASEs. The percentage of positive and negative correlations of RBP and DASE in each group was showed. **G** Correlation analysis between immune cells and DASEs. Number of DASEs positively or negatively correlated with the ratio of 21 immune cells in each infection group was showed. Up and downregulated DASEs were inspected separately.

length related to those DASEs in each splice type (Supplementary Fig. S1C), and found the intron length related to the alternative splicing events varies greatly among different infection groups.

Alternative splicing is involved in pathological and physiological functions (Lin et al., 2015; Pozzi et al., 2020). We performed pathway enrichment analysis to examine the genes containing alternative splicing events, and the number of top biological processes enriched by DASEs of five infection groups were shown in Fig. 1C. We observed DASEs in all groups were enriched in several pivotal pathways such as metabolic process (average 109 and 160 gene sets in up and downregulated DASEs, respectively), response to stimulus (average 67 and 109 gene sets in up and downregulated DASEs, respectively) and immune system process (average 46 and 63 gene sets in up and downregulated DASEs, respectively). The number of enriched DASEs in top pathways were shown in Fig. 1D. Counting the number of DASEs in the top enriched pathways established, metabolic process contained the most of DASEs (average 47.9% of upregulated DASEs and 52.7% of downregulated DASEs across five groups), as well as response to stimulus (average 32.4% of upregulated DASEs and 43.4% of downregulated DASEs), localization (average 30.1% of upregulated DASEs and 36.6% of downregulated DASEs), immune system (average 23.8% of upregulated DASEs and 28.8% of downregulated DASEs) and viral processes (average 9.3% of upregulated DASEs and 6.8% of downregulated DASEs). The enrichments of specific metabolic and immune system processes in five groups are further analyzed in Supplementary Fig. S2, Table S2, and Table S3.

RNA binding proteins (RBPs)/splicing factors (SFs) are key regulators in alternative splicing processes (Maniatis and Tasic, 2002; Li et al., 2019). To better understand the underlying regulation of splicing after infection, we performed a correlation analysis between RBP and DASEs. Global analysis revealed hundreds of RBPs are significantly correlated with DASEs in all groups ($|r| > 0.6$, adjusted P-value <0.05) (Fig. 1E). For example, in bacterial pneumonia, we observed 2609 positive correlations between 601 RBPs and 183 upregulated DASEs, as well as 2603 negative correlations between 918 RBPs and 236 upregulated DASEs. In SARS-CoV-2 (Severe), 462 positive correlations between 224 RBPs and 154 downregulated DASEs and 1327 negative correlations between 187 RBPs and 333 downregulated DASEs were observed (Supplementary Table S4). The percentage of positive and negative correlations of RBP and DASE in each group were shown in Fig. 1F.

We further identified the top RBPs which were correlated with a large number of DASEs in each infection group. Several common and specific splicing factors/RBPs established a significant correlation with DASEs. For example, in bacterial pneumonia, splicing factors ENOX1, RBFOX3, ELAVL2, SRSF9 and six other RBPs were significantly correlated with the largest number of upregulated DASEs. One splicing factor family CELF was frequently identified as correlated to DASEs in different infection groups. For example, CELF5, CELF4 and CELF6 were the top SFs correlated with upregulated DASEs of seasonal coronvirus, SARS-CoV-2 (Mild) and SARS-CoV-2 (Severe), respectively. CELF6 was also the top SF correlated with downregulated DASEs of bacterial pneumonia. METTL16 and RPS19 are the top RBPs correlated with up and downregulated DASEs in SARS-CoV-2 (Mild). ADARB2 is the top RBP correlated with up and downregulated DASEs in SARS-CoV-2 (Severe) (Supplementary Fig. S3). All results indicate a number of RBPs are potentially involved in the process of alternative splicing in pathogen infections.

Dysregulation of cell abundance is one of the consequences after virus infection (Wherry et al., 2007; Scott-Browne et al., 2016; Vabret et al., 2020). However, the involvement of alternative splicing in this process was less known. We estimated the ratio of 21 types of immune cells in five infection groups and performed correlation analysis between cell abundance and DASEs. Number of DASEs positively or negatively correlated with the ratio of 21 immune cell were shown in Fig. 1G. Results indicated 72, 74, 59, 42 and 77 DASEs were significantly positively correlated with 8, 14, 11, 7 and 13 types of immune cells in SARS-CoV-2 (Severe), SARS-CoV-2 (Mild), influenza, seasonal coronavirus and bacterial pneumonia, respectively. In addition, 180, 150, 170, 52 and 136 DASEs were notably negatively correlated with 9, 17, 15, 11 and 17 types of immune cells in SARS-CoV-2 (Severe), SARS-CoV-2 (Mild), influenza, seasonal coronavirus and bacterial pneumonia, respectively (Fig. 1G and Supplementary Table S5).

Special cell types were observed in correlation with DASEs in different infections. For example, in SARS-CoV-2 (Severe), activated NK cells were remarkablly positively correlated with 44 DASEs (30 upregulated and 14 downregulated DASEs), and negatively correlated with 120 DASEs (4 upregulated and 116 downregulated DASEs). In SARS-CoV-2 (Mild), Macrophages M2 were significantly positively correlated with 14 DASEs (10 upregulated and 4 downregulated DASEs), and negatively correlated with 27 DASEs (16 upregulated and 11 downregulated DASEs). In influenza, T cells follicular helper (TFH) were markedly positively correlated with 21 DASEs (13 upregulated and 8 downregulated DASEs), and negatively correlated with 30 DASEs (14 upregulated and 16 downregulated DASEs). In seasonal coronavirus, plasma cells were significantly positively correlated with 22 DASEs (10 upregulated and 12 downregulated groups), and negatively correlated with 25 DASEs (11 upregulated and 15 downregulated groups). In bacterial pneumonia, eosinophils were observably positively correlated with 24 DASEs (20 upregulated and 4 downregulated DASEs), and negatively correlated with 24 DASEs (12 upregulated and 14 downregulated DASEs) (Supplementary Fig. S4 and Table S5). Results indicate the involvement of alternative splicing in the regulation of cell abundance, during pathogen infections.

The overlaps of differential alternative spliced genes (DASGs) and differential expressed genes (DEGs) were examined in each of the five infection groups compared to the healthy controls. Notably, a larger number of genes that were affected in both transcription and post-transcription splicing were observed in SARS-CoV-2 (Severe) group, compared with SARS-CoV-2 (Mild) group (Supplementary Figs. S5A and C and Table S6). As shown in Supplementary Figs. 5B and 1756 DASGs were induced in SARS-CoV-2 (Severe) group of which, surprisingly, only 79 exhibit significant differences in mRNA levels (Supplementary Fig. S5C). To focus on the functions of these overlapped genes, GO analysis was performed and showed that differentially spliced genes with changes in abundance were mainly enriched in regulation of viral life cycle, viral process and negative regulation of viral genome replication in SARS-CoV-2 (severe) and SARS-CoV-2 (Mild) group (Supplementary Figs. S5B and D and Table S7). The similar phenomenon occurred in the cases of other three infection groups (Supplementary Figs. 5E–J). The alternative spliced genes and differential expressed genes were quite different in each group, which was consistent with many previous studies (Gazzara et al., 2017; Thompson et al., 2020). In bacterial and influenza groups, the overlapped genes were commonly enriched in cytoplasmic translation, peptide biosynthetic process and translation pathway, while in seasonal coronaviruses group, these genes were enriched in peptide metabolic process, cellular macromolecule biosynthetic process and cellular amide metabolic process. The data showed larger amounts of alternative spliced genes in mild SAR-CoV-2, severe SAR-CoV-2, influenza group while much less genes in bacterial and seasonal coronaviruses groups. In bacterial group, only 471 genes underwent alternative splicing, but the overlap of these genes and DEGs accounted for 29.5% (139 genes). On the whole, pathogens cause functionally distinct landscapes of host transcriptional responses and splicing programs.

The whole blood samples are rich in cell types, which can better reflect the overall health status. The whole blood transcriptome is also an important indicator which could reflect the post-infection changes of circulatory system, further helping researchers to evaluate the effects of infections. Thus, many previous works used the whole blood transcriptome to inspect the expression or immune changes among the pathology of COVID-19 (Galbraith et al., 2021; Wu et al., 2021; COvid-19 Multi-omics Blood ATlas COMBAT Consortium, 2022), including the datasets used in this work (McClain et al., 2021; Wang et al., 2021). Our research is the first try of global exploration of alternative splicing changes in COVID-19 and relevant respiratory diseases and provides a

landscape profile on the specificities and similarities among alternative splicing events in different respiratory diseases. However, the changes of whole blood are possibly not directly related to the pathogen infections. It might be possible that the alternative splicing pattern of changes were related to the seriousness extent of infections, which are indicated in our analysis between SARS-CoV-2 (Mild) and SARS-CoV-2 (Severe) groups in respect of distribution features, functional enrichment of these events, RBP-splicing regulatory, as well as cell abundance correlations. This is worthy of our consideration in the future work. It will require analysis of a larger number of clinical cases based on samples collected across the progression of the diseases and from cells or tissues of the respiratory origin. In general, although some practical factors are insufficient, such as sample size, our work revealed the global changes and characteristics of alternative splicing events during pathogen infections, providing a new way to trace the host responses in respiratory diseases.

Footnotes

This work was supported by the National Key Research and Development Plan of China (Grant No. 2021YFC2300700). The authors declare that they have no conflicts of interest. This article does not contain any studies with human or animal subjects performed by any of the authors.

RNA-Seq data from the previous public dataset (McClain et al., 2021) were obtained from the GEO database (http://www.ncbi.nlm.nih.gov/geo/) (Barrett et al., 2013) (GSE161731). All the data generated during the current study are included in the manuscript. For more information, please contact che@whu.edu.cn (C. He).

Supplementary data to this article can be found online at https://doi.org/10.1016/j.virs.2023.01.007.

References

Ashraf, U., Benoit-Pilven, C., Lacroix, V., Navratil, V., Naffakh, N., 2019. Advances in analyzing virus-induced alterations of host cell splicing. Trends Microbiol. 27, 268–281.

Barrett, T., Wilhite, S.E., Ledoux, P., Evangelista, C., Kim, I.F., Tomashevsky, M., Marshall, K.A., Phillippy, K.H., Sherman, P.M., Holko, M., Yefanov, A., Lee, H., Zhang, N., Robertson, C.L., Serova, N., Davis, S., Soboleva, A., 2013. NCBI GEO: archive for functional genomics data sets–update. Nucleic Acids Res. 41, D991–995.

Bonenfant, G., Meng, R., Shotwell, C., Badu, P., Payne, A.F., Ciota, A.T., Sammons, M.A., Berglund, J.A., Pager, C.T., 2020. Asian Zika virus isolate significantly changes the transcriptional profile and alternative RNA splicing events in a neuroblastoma cell line. Viruses 12, 510.

Gazzara, M.R., Mallory, M.J., Roytenberg, R., Lindberg, J.P., Jha, A., Lynch, K.W., Barash, Y., 2017. Ancient antagonism between CELF and RBFOX families tunes mRNA splicing outcomes. Genome Res. 27, 1360–1370.

COvid-19 Multi-omics Blood ATlas (COMBAT) Consortium, 2022. A blood atlas of COVID-19 defines hallmarks of disease severity and specificity. Cell 185, 916–938.e958.

Duriez, M., Mandouri, Y., Lekbaby, B., Wang, H., Schnuriger, A., Redelsperger, F., Guerrera, C.I., Lefevre, M., Fauveau, V., Ahodantin, J., Quetier, I., Chhuon, C., Gourari, S., Boissonnas, A., Gill, U., Kennedy, P., Debzi, N., Sitterlin, D., Maini, M.K., Kremsdorf, D., Soussan, P., 2017. Alternative splicing of hepatitis B virus: a novel virus/host interaction altering liver immunity. J. Hepatol. 67, 687–699.

Fox-Walsh, K.L., Dou, Y., Lam, B.J., Hung, S.P., Baldi, P.F., Hertel, K.J., 2005. The architecture of pre-mRNAs affects mechanisms of splice-site pairing. Proc. Natl. Acad. Sci. U. S. A. 102, 16176–16181.

Galbraith, M.D., Kinning, K.T., Sullivan, K.D., Baxter, R., Araya, P., Jordan, K.R., Russell, S., Smith, K.P., Granrath, R.E., Shaw, J.R., Dzieciatkowska, M., Ghosh, T., Monte, A.A., D'Alessandro, A., Hansen, K.C., Benett, T.D., Hsieh, E.W., Espinosa, J.M., 2021. Seroconversion stages COVID19 into distinct pathophysiological states. Elife 10, e65508.

Kremsdorf, D., Lekbaby, B., Bablon, P., Sotty, J., Augustin, J., Schnuriger, A., Pol, J., Soussan, P., 2021. Alternative splicing of viral transcripts: the dark side of HBV. Gut 70, 2373–2382.

Lee, Y., Rio, D.C., 2015. Mechanisms and regulation of alternative pre-mRNA splicing. Annu. Rev. Biochem. 84, 291–323.

Li, S., Hu, Z., Zhao, Y., Huang, S., He, X., 2019. Transcriptome-wide analysis reveals the landscape of aberrant alternative splicing events in liver cancer. Hepatology 69, 359–375.

Li, D., Su, M., Sun, P.P., Guo, W.P., Wang, C.Y., Wang, J.L., Wang, H., Zhang, Q., Du, L.Y., Xie, G.C., 2020. Global profiling of the alternative splicing landscape reveals transcriptomic diversity during the early phase of enterovirus 71 infection. Virology 548, 213–225.

Lin, W., Zhu, C., Hong, J., Zhao, L., Jilg, N., Fusco, D.N., Schaefer, E.A., Brisac, C., Liu, X., Peng, L.F., Xu, Q., Chung, R.T., 2015. The spliceosome factor SART1 exerts its anti-HCV action through mRNA splicing. J. Hepatol. 62, 1024–1032.

Maniatis, T., Tasic, B., 2002. Alternative pre-mRNA splicing and proteome expansion in metazoans. Nature 418, 236–243.

McClain, M.T., Constantine, F.J., Henao, R., Liu, Y., Tsalik, E.L., Burke, T.W., Steinbrink, J.M., Petzold, E., Nicholson, B.P., Rolfe, R., Kraft, B.D., Kelly, M.S., Saban, D.R., Yu, C., Shen, X., Ko, E.M., Sempowski, G.D., Denny, T.N., Ginsburg, G.S., Woods, C.W., 2021. Dysregulated transcriptional responses to SARS-CoV-2 in the periphery. Nat. Commun. 12, 1079.

Pozzi, B., Bragado, L., Mammi, P., Torti, M.F., Gaioli, N., Gebhard, L.G., Garcia Sola, M.E., Vaz-Drago, R., Iglesias, N.G., Garcia, C.C., Gamarnik, A.V., Srebrow, A., 2020. Dengue virus targets RBM10 deregulating host cell splicing and innate immune response. Nucleic Acids Res. 48, 6824–6838.

Scott-Browne, J.P., Lopez-Moyado, I.F., Trifari, S., Wong, V., Chavez, L., Rao, A., Pereira, R.M., 2016. Dynamic changes in chromatin accessibility occur in CD8(+) T cells responding to viral infection. Immunity 45, 1327–1340.

Thompson, M.G., Dittmar, M., Mallory, M.J., Bhat, P., Ferretti, M.B., Fontoura, B.M., Cherry, S., Lynch, K.W., 2020. Viral-induced alternative splicing of host genes promotes influenza replication. Elife 9, e55500.

Tomezsko, P.J., Corbin, V.D.A., Gupta, P., Swaminathan, H., Glasgow, M., Persad, S., Edwards, M.D., McIntosh, L., Papenfuss, A.T., Emery, A., Swanstrom, R., Zang, T., Lan, T.C.T., Bieniasz, P., Kuritzkes, D.R., Tsibris, A., Rouskin, S., 2020. Determination of RNA structural diversity and its role in HIV-1 rna splicing. Nature 582, 438–442.

Vabret, N., Britton, G.J., Gruber, C., Hegde, S., Kim, J., Kuksin, M., Levantovsky, R., Malle, L., Moreira, A., Park, M.D., Pia, L., Risson, E., Saffern, M., Salome, B., Esai Selvan, M., Spindler, M.P., Tan, J., van der Heide, V., Gregory, J.K., Alexandropoulos, K., Bhardwaj, N., Brown, B.D., Greenbaum, B., Gumus, Z.H., Homann, D., Horowitz, A., Kamphorst, A.O., Curotto de Lafaille, M.A., Mehandru, S., Merad, M., Samstein, R.M., Sinai Immunology Review P, 2020. Immunology of COVID-19: current state of the science. Immunity 52, 910–941.

Wang, L.Y., Balmat, T.J., Antonia, A.L., Constantine, F.J., Henao, R., Burke, T.W., Ingham, A., McClain, M.T., Tsalik, E.L., Ko, E.R., Ginsburg, G.S., DeLong, M.R., Shen, X.L., Woods, C.W., Hauser, E.R., Ko, D.C., 2021. An atlas connecting shared genetic architecture of human diseases and molecular phenotypes provides insight into COVID-19 susceptibility. Genome Med. 13, 83.

Wherry, E.J., Ha, S.J., Kaech, S.M., Haining, W.N., Sarkar, S., Kalia, V., Subramaniam, S., Blattman, J.N., Barber, D.L., Ahmed, R, 2007. Molecular signature of CD8+ T cell exhaustion during chronic viral infection. Immunity 27, 670–684.

Wu, P., Chen, D., Ding, W., Wu, P., Hou, H., Bai, Y., Zhou, Y., Li, K., Xiang, S., Liu, P., Ju, J., Guo, E., Liu, J., Yang, B., Fan, J., He, L., Sun, Z., Feng, L., Wang, J., Wu, T., Wang, H., Cheng, J., Xing, H., Meng, Y., Li, Y., Zhang, Y., Luo, H., Xie, G., Lan, X., Tao, Y., Li, J., Yuan, H., Huang, K., Sun, W., Qian, X., Li, Z., Huang, M., Ding, P., Wang, H., Qiu, J., Wang, F., Wang, S., Zhu, J., Ding, X., Chai, C., Liang, L., Wang, X., Luo, L., Sun, Y., Yang, Y., Zhuang, Z., Li, T., Tian, L., Zhang, S., Zhu, L., Chang, A., Chen, L., Wu, Y., Ma, X., Chen, F., Ren, Y., Xu, X., Liu, S., Wang, J., Yang, H., Wang, L., Sun, C., Ma, D., Jin, X., Chen, G., 2021. The trans-omics landscape of COVID-19. Nat. Commun. 12, 4543.

Zheng, H.Y., Xu, M., Yang, C.X., Tian, R.R., Zhang, M., Li, J.J., Wang, X.C., Ding, Z.L., Li, G.M., Li, X.L., He, Y.Q., Dong, X.Q., Yao, Y.G., Zheng, Y.T., 2020. Longitudinal transcriptome analyses show robust t cell immunity during recovery from COVID-19. Signal Transduct. Targeted Ther. 5, 294.